Turbulent Flow Field Structure of Initially Asymmetric Jets

Kyung-Hoon Kim*, Bong-Whan Kim
College of Mechanical and Industrial System Engineering., Institute of Laser Engineering, Kyung-Hee University
Suk-Woo Kim
Hyundae Construction Co.

The near field structure of round turbulent jets with initially asymmetric velocity distributions is investigated experimentally. Experiments are carried out using a constant temperature hot-wire anemometry system to measure streamwise velocity in the jets. The measurements are undertaken across the jet at various streamwise stations in a range starting from the jet exit plane and up to a downstream location of twelve diameters. The experimental results include the distributions of mean and instantaneous velocities, vorticity field, turbulence intensity, and the Reynolds shear stresses. The asymmetry of the jet exit plane was obtained by using circular cross-section pipes with a bend upstream of the exit. Three pipes used here include a straight pipe, and 90 and 160 degree-bend pipes. Therefore, at the upstream of the pipe exit, secondary flow through the bend and mean streamwise velocity distribution could be controlled by changing the curvature of pipes. The jets into the atmosphere have two levels of initial velocity skewness in addition to an axisymmetric jet from a straight pipe. In case of the curved pipe, a six diameter-long straight pipe section follows the bend upstream of the exit. The Reynolds number based on the exit bulk velocity is 13,400. The results indicate that the near field structure is considerably modified by the skewness of an initial mean velocity distribution. As the skewness increases, the decay rate of mean velocity at the centerline also increases.

Key Words : Asymmetric Jet, Hot-wire Anemometry, Turbulence Intensity, Reynolds Shear Stress, Vorticity

Nomenclature

D : Pipe diameter
K : Dean number $=(R/R_C)^{0.5}Re$
R : Pipe radius
R_c : Radius of curvature of pipe bend
Re : Reynolds number $=(U_bD)/\nu$
U : Axial coordinate
U_b : Mean bulk velocity at exit
U_m : Maximum of U
U_o : Jet exit maximum velocity
u′ : rms of fluctuating streamwise velocity
V : Lateral coordinate mean velocity
v′ : rms of fluctuating cross-stream velocity
u'_{cl} : u′ on the center-line
v'_{cl} : v′ on the center-line
$\overline{u'v'}$: Reynolds shear stress
x : Axial coordinate measured from pipe exit
y : Lateral coordinate on jet symmetry plane
z : Coordinate normal to the jet symmetry plane
Ω_z : Vorticity component normal to jet symmetry plane
μ_t : Turbulent viscosity

* Corresponding Author,
E-mail : kimkh@khu.ac.kr
TEL : +82-31-201-2509 ; **FAX** : +82-31-202-8106
College of Mechanical and Industrial System Engineering, Institute of Laser Engineering, Kyung-Hee University 1, Seochon-ri, Kihung-up, Yongin-si, Kyunggi-do 449-701, Korea. (Manuscript **Received** November 27, 1999; **Revised** August 21, 2000)

1. Introduction

The near field structure of round turbulent jets with three-dimensional(or asymmetric) initial velocity distributions is investigated experimentally. Although turbulent jets have been extensively investigated for decades, the effort has been concentrated on plane symmetric and axisymmetric jets(Sforza et al., 1966 ; Trentacoste and Sforza, 1967 ; Bradbury, 1965 ; Townsend, 1956 ; Rockwell and Dec, 1972 ; Namer and Otugen, 1988). As a result, little is known on asymmetric turbulent jets. In practice, there are examples where a jet emerges from a source with a non-symmetric velocity profile(e. g. jet ejector, gas leaks from cracks in piping, etc.) (Birch et al., 1978 ; Chevray and Tutu, 1978 ; Dimotakis et al., 1983 ; Papanicolaou and List, 1988). These flows show significantly different flow properties in the initial development region than their symmetric counterparts exhibit. The initially non-symmetric (skewed) mean shear distribution is quite likely to affect the evolution of the turbulent flow field and modify overall momentum mixing. Therefore, if asymmetric jets prove to have significant gradients of turbulent transport across the shear layer, they may be used as mixing control and enhancement mechanisms.

In general, the flow field of plane symmetric (or round axisymmetric) turbulent jets are divided into two regions(Ricou and Spalding, 1990 ; Hussain and Tso, 1989 ; Oosthuizen, 1983 ; Shlien, 1987 ; Gibson, 1963 ; Krothapalli et al., 1981 ; Hussain and Husain, 1989 ; Trentacoste and Sforza, 1968) : The initial region(or the near field region) and self-preserving region(or far field region). The initial region is the zone immediately downstream of the nozzle exit where the flow experiences a sudden change in boundary conditions from a confined flow to a free shear layer flow. The downstream growth characteristics of the turbulent jet are a strong function of flow pattern in the initial region. In this region, for jets with uniform initial velocity distribution, the subsequent growth and dilution is determined by the production of large scale vortices and their consequent pairing, growth, instability, and destruction. However, the jet flow becomes fully developed with turbulent energy in near equilibrium and the mean and turbulent velocity profiles showing self-preserving characteristics.

Investigations have also been reported in three-dimensional jets emerging from rectangular as well as elliptic orifices(Yu and Kim, 1996 ; Kwon, 1998 ; Townsend, 1966). The rectangular jets are characterized by three regions: The initial region which includes the potential core, the two-dimensional jet type region, and the axisymmetric jet type region. The two latter regions are identified by the corresponding velocity decay rates. The elliptic jet can be viewed as the intermediate case between the axisymmetric and the plane symmetric jet. In the case of elliptic jet, flow development is strongly controlled by the dynamics of the initial vortex ring and high mixing rate can be achieved at some optimum major-to-minor axis ratio.

All jet forms mentioned above have one common characteristic: The distribution of mean flow properties are either axisymmetric about the jet center-line or symmetric on the two sides of the center-plane parallel to the sides of the jet. Therefore, for these jet forms the turbulence field and the associated transport properties are also symmetric or axisymmetric about the jet axis.

The present investigation aims at studying the initial flow geometry(i. e. mean velocity field) effects rather than the facility geometry on the evolution and three-dimensional behavior of the turbulent free shear layer. While the orifice itself is axisymmetric in geometry, the flow distribution is asymmetric at the source. Another distinction that needs to be borne in mind is that in the present jet studies the initial flow is a shear layer and no potential core exists in the jet downstream zone.

2. Experimental Technique

2.1 Apparatus and instrumentation

High pressure air is supplied through a regulator and a control valve into an 203mm diameter and 610mm long cylindrical settling chamber,

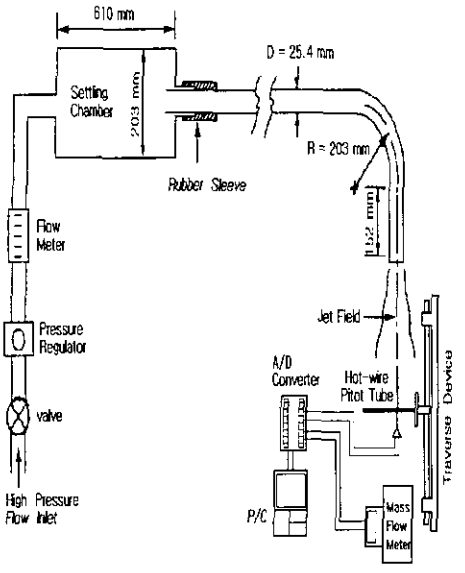

Fig. 1 Schematic of experimental set-up

shown in Fig. 1.

The static pressure in the chamber is monitored via a Validyne variable reluctance pressure tranceducer (Model DP 7) and displayed through Validyne Model CD23 digital indicator during measurements. In order to ensure the constant mass flow rate of air, the pressure head in the settling chamber is kept at 22mm of water for each experiment and its variation is under 0. 25mm of water. At the downstream end of the chamber, a 25.4mm diameter steel pipe is coupled using an air tight rubber coupling. The pipe is inserted into the settling chamber about 50mm to ensure an axisymmetric inlet into the pipe. While a straight pipe is utilized to measure the axisymmetric jet, which is referred to as Case I, pipes with two degrees of bend before the exit are used for asymmetric turbulent jets. For each of these pipes, a fixed mean radius of curvature(203mm) is applied for the bend before the exit. The Reynolds number based on the diameter of the pipe and the exit mean bulk velocity is 13,400. The level of skewness of streamwise velocity at the jet exit can be controlled by the angle of turn through the bend. In the present experiments, bend angles of 90 degree(Case Ⅱ) and 160 degree (Case Ⅲ) are used. For each bend pipe, a 5 diameter long straight section is followed by the bend in order to recover the pressure from perturbation through the bend. For the straight pipe, the ratio of length to diameter is 100 to ensure a fully developed flow at the exit. For the curved pipes, a 110 diameter section precedes the bend. Both single and cross type hot-wire sensors are used for hot-wire measurements. The diameter and length of tungsten sensors are 5 micron and 1. 2mm, respectively. The sensors are calibrated in a standard calibration air jet. The TSI Model 1050 constant temperature hot-wire anemometers equipped with linearizers are used and adjusted to a frequency response of about 30kHz. For data acquisition, a 80586 architecture personal computer is used. The instantaneous signals from hot -wire sensors are digitized by a MetraByte DAS -16F, 12 bit resolution A/D converter. Mean velocity, turbulence intensity and Reynolds stress are calculated and stored on a 2Gb hard disk. The data is obtained through records of 20 seconds with a rate of 200 samples per second. The uncertainty level for velocity in the current study is $\pm$2. 1%.

A traversing mechanism is used to allow traverses along the horizontal(y) and vertical(z) directions for jet cross section measurements at different axial(x) positions. This two-axis traversing mechanism is mounted on an adjustable rail, which is aligned parallel to the jet axis(x). A rotary dial is fixed to the y-z plane traversing mechanism to record the linear displacement of linear motion and the linear displacement per revolution is 0.424mm. The positioning accuracy of the y-z plane traversing mechanism is 0.01 mm while the maximum deviation along x direction is 0.4mm.

2.2 Procedure

The experimental investigation is divided into two stages. The first(preliminary) stage is to place the hot-wire sensor precisely on the jet axis and to provide the information that characterizes the turbulent jet flows. In order to obtain information on the jet initial conditions, velocity measurements are on the y-z plane at the jet exit of each pipe. The Reynolds number is calculated and Dean number, which is defined as k=

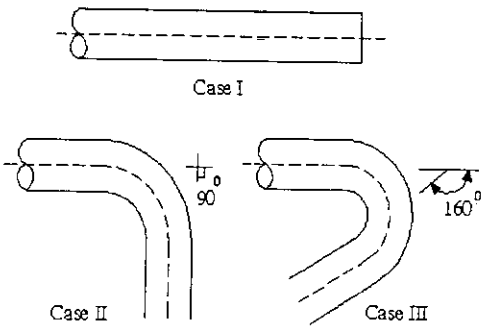

Fig. 2 Nozzle configuration of Case Ⅰ, Ⅱ, Ⅲ

$(R/R_C)^{0.5}Re$, is also calculated. In the present investigation, Dean number is fixed at 3,350. The distribution of pressure along the circumference of the pipe exit is measured using a pitot tube. The bulk velocity is determined by numerical integration of axial mean velocity at the jet exit. The primary purpose of preliminary measurements is to determine a proper sampling rate and to maintain the same flow characteristics for each pipe. This is accomplished by measuring the mean axial velocity along the y-z plane at the pipe exit and adjusting a control valve. Therefore, the Reynolds number is kept constant for Case Ⅰ, Ⅱ, and Ⅲ (which refer to jets emerging from straight, 90° bend and 160° bend pipes, respectively; Fig. 2). Next, velocity measurements are made in the axisymmetric jet emerging from the straight pipe in order to form a basis for comparison with the asymmetric jets. A cross type hot-wire sensor is used to measure the mean velocity profile at every diameter along the downstream direction. A single hot-wire sensor is also used to obtain the two-dimensional axisymmetry at various streamwise locations. The first asymmetric jet (Case Ⅱ) is obtained by allowing the upstream pipe flow through a 90 degree bend before the jet exit. This way, the axisymmetric axial momentum distribution in the pipe is perturbed. The second asymmetric jet (Case Ⅲ) is obtained through a 160 degree bend pipe with the same radius of curvature rendering a stronger asymmetry of initial jet characteristics. In all three cases, the jets are emerged into still air, and the mean bulk velocity is 8.5m/s. The measurements of axial mean velocity and turbulence intensity are made

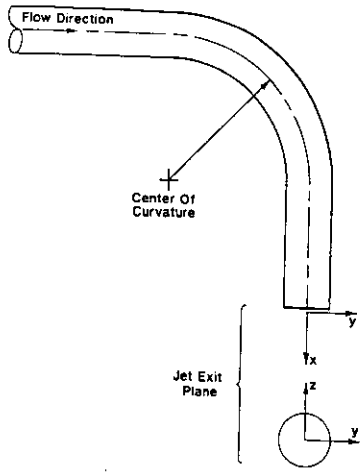

Fig. 3 Coordinate system for flow

on the x-y plane along the centerline of a pipe jet symmetry plane. The coordinate system is shown in Fig. 3. Here, x is the streamwise coordinate along the jet axis while y and z are the cross-stream coordinates parallel and normal to the plane of a pipe bend. A Fortran program is implemented to calculate the mean velocity, turbulence intensity, and Reynolds stress from the instantaneous velocity records. The velocity is normalized by the mean bulk velocity U_b, which is determined by numerical integration of axial velocity obtained at the jet exit. For each bend pipe, instantaneous velocity measurements are taken at streamwise stations up to 12 diameter downstream from the exit plane. The measurements are taken along the cross-stream direction up to a radial distance where U/U_b is less than 0.5. As it will be discussed in the next section, the maximum and the minimum of the mean streamwise velocity occur along the y-axis in Case Ⅰ, Ⅱ, and Ⅲ. This is accompanied with the maxima and minima of mean shear which also occur on the same axis. The jet exit turbulence intensity distributions are similar to those for the mean velocity in that they show symmetry about the x-y plane. In the present investigation, therefore, the x-y plane is viewed as the symmetry plane ($z=0$). Further measurements of velocity are carried out only on the symmetry plane to focus on the development of the initially asymmetric velocity distribution.

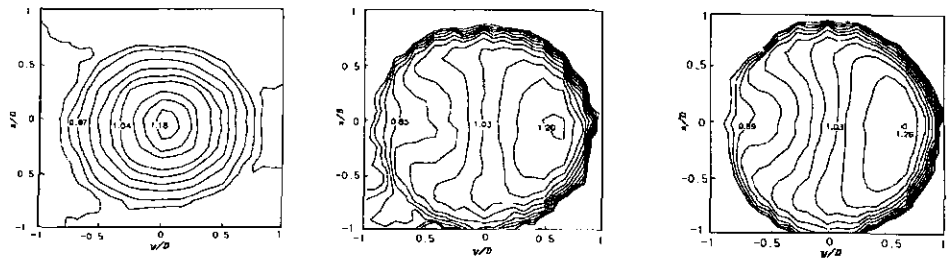

Case I Case II Case III

Fig. 4 Constant velocity contours at the jet exit for Case Ⅰ, Ⅱ, Ⅲ

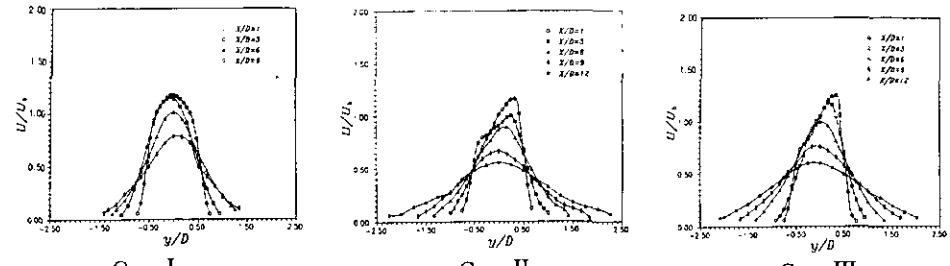

Case I Case II Case III

Fig. 5 Mean streamwise velocity profiles for Case Ⅰ, Ⅱ, Ⅲ

3. Results and Discussion

3.1 Mean velocity

Case Ⅰ in Fig. 4 gives the mean velocity distribution at the exit of the straight pipe where the velocity profile is symmetric about the x-y plane. Case Ⅱ and Ⅲ in Fig. 4 show the velocity profiles at the exit of 90° and 160° bend pipes where the velocity is normalized by the mean bulk velocity U_b. In both cases, the velocity distributions at the exit plane is asymmetric and the maximum velocity is located at the outer edge of the jet. This is the result because of the imbalance between the centrifugal forces and radial pressure gradient in the curved section of the pipe upstream of the exit. The fluids at the pipe axis move toward the outer edge of the pipe, while the fluids near the top and bottom walls move toward the inner side. This essentially accounts for the reason why the maximum velocity occurs at the outer region of the jet. Under the influences of the streamline curvature and angle of the bend, the maximum velocity is located further away from the jet center-line in Case Ⅲ in comparison that

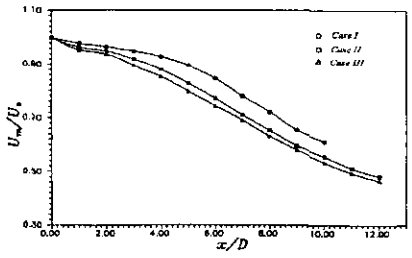

Fig. 6 Axial distribution of maximum mean streamwise velocity

with Case Ⅱ. In Case Ⅱ, the maximum streamwise mean velocity occurs at y/D=0.61, while it occurs at y/D=0.67 in Case Ⅲ. The maximum streamwise mean velocities normalized by U_b, are 1.1763, 1.2034, and 1.2622 for the straight pipe, and 90° and 160° bend pipes, respectively. These results show that the maximum streamwise velocity increases as the angle of bend increases. Therefore, the strength of secondary motion and the degree of skewness can be determined in terms of the curvature and angle of the bend. Case Ⅰ through Ⅲ in Fig. 5 show the streamwise mean velocity distributions at several selected axial locations. case Ⅱ and Ⅲ illustrate

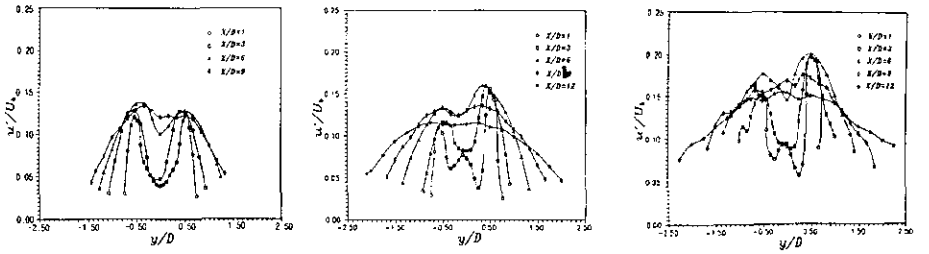

Case I Case II Case III

Fig. 7 u′ profiles for Case Ⅰ, Ⅱ, Ⅲ

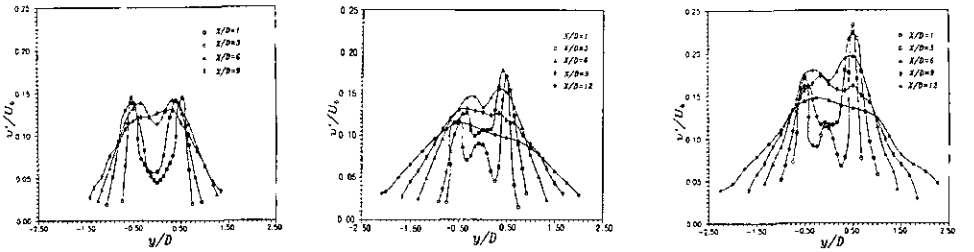

Case I Case II Case III

Fig. 8 v′ profiles for Case Ⅰ, Ⅱ, Ⅲ

the streamwise velocity skewness of 90° and 160° bend pipes. These initially asymmetric jets show higher decay rates of the maximum velocity compared to the axisymmetric jet (Fig. 6). The decay rates become equal for all three jets at an axial distance of x/D=7. As the skewness level of initial jet velocity distribution is increased, the velocity decay rate increases for x/D<7. It is difficult to measure accurately the cross-stream mean velocity with a hot-wire sensor due to small magnitudes of velocity encountered. Although the accurate alignment of a hot-wire to the axis of jet is helpful to minimize the experimental error, there still exists large error margins in the distribution of the entrainment velocity. Therefore, the results for cross-stream mean velocity are not presented in this report. However, the average fluctuating velocity, v′, is much larger than its mean counterpart, V, as will be seen in the following section.

3.2 Turbulence intensity

Case Ⅰ through Ⅲ in Fig. 7 illustrate the streamwise turbulence intensify distributions in jets emerging from straight, 90° and 160° bend pipes. Case Ⅰ through Ⅲ in Fig. 8 are for the turbulent velocity fluctuation distributions in the cross-stream direction. Each distribution of turbulence fluctuation is normalized by U_b. In the case of straight pipe jet, u′ and v′ are symmetric about the x-axis as expected, and their center-line values remain almost constant and equal beyond x/D=6, which also verify the experimental results of Corrsin (Townsend, 1956) and Gibson (Trentacoste and Sforza, 1968) who observed near isotropy of turbulence at the jet axis. These results may be expected since there is no production of turbulence at the x-axis especially in the view of absence of a potential core, and the turbulence presence is only due to transport by the mean turbulence motion. It is also observed that the near-field distribution of v′ has, on the average, slightly higher maximum values than those for u′. Yet, u′ profiles spread faster than the profiles for v′ with increasing axial distance. Overall, the u′ and v′ are quite comparable in magnitude perhaps limiting to a global isotropy of turbulence at least in the initial jet zone. In Case Ⅱ, u′ and v′ have non-symmetric distributions of turbulence due to the non-symmetric mean shear distribution. At the exit, the normalized minimum u′ and v′ are of 0.0047 and 0.0053

at y/D=0.3339. These values become larger further downstream of the flow. At the jet exit plane, the magnitudes of u′ and v′ in Case Ⅱ are about 23% larger than those in Case Ⅰ, the difference becomes smaller further down-stream. In Case Ⅲ, the maximum values of u′ and v′ are much greater than those of Case Ⅰ and Ⅱ. The maximum values of u′ and v′ in Case Ⅲ are further away from the jet center-line in comparison that with Case Ⅰ and Ⅱ. The initial distributions of u′ and v′ are asymmetric due to non-symmetric mean shear distribution. Since the mean shear distribution is influenced by skewness of mean velocity, u′ and v′ are higher in the outer region than in the inner region of the jet. Figures 9 and 10 show the axial distributions of u′ and v′ at the center-line of the jets.

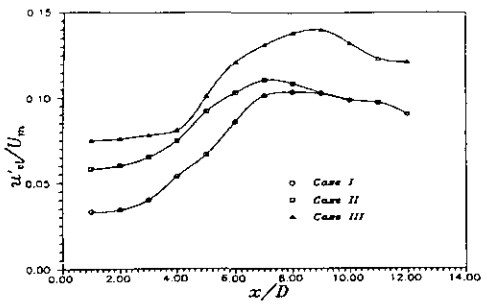

Fig. 9 *Axial distribution of u′ along the center-line of jet*

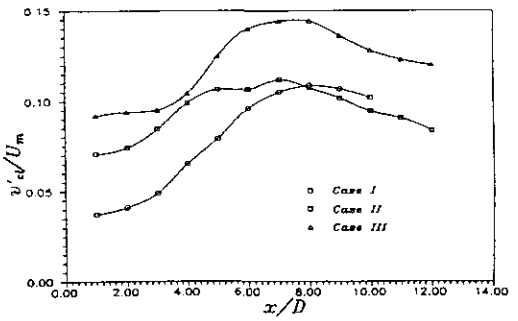

Fig. 10 Axial distribution of v′ along the center-line of jet

It shows that u′ in Case Ⅲ is about 30% larger at the jet exit plane than that of Case Ⅱ. In Case Ⅱ, both profiles of u′ and v′ show the rapid increase rates up to x/D=7, and the smooth decay rates are shown after that. In Case Ⅲ, however, the values of u′ and v′ increase rapidly up to x/D=8 and then decrease smoothly. As the skewness increases, u′ and v′ increases. Also, the overall turbulence increases with x/D in the initial region, up to about x/D=7 due to the diffusion mechanism in jets. The rapid diffusion leads to an increase of turbulence along the centerline, making the jet stable to the growth of large eddies in the initial region. However, the turbulence is too large to permit the growth of large eddies, diffusion is weak and the turbulence decreases until the jet is unstable to the development of large eddies. Accordingly, the turbulence in Case Ⅰ, Ⅱ and Ⅲ decreases beyond x/D=7.

3.3 Reynolds shear stress

As Case Ⅰ in Fig. 11 illustrates, the profiles of absolute values of Reynolds shear stress, $\overline{u'v'}$, are symmetric along the x-axis in Case Ⅰ. At the exit, the normalized maximum value of shear stress is 0.9, located at y/D=0.2671 and decrease with downstream distance. However, as expected, at y/D=0, the value of shear stress is always almost zero giving credence to the current measurements of $\overline{u'v'}$. Case Ⅱ gives the shear stress

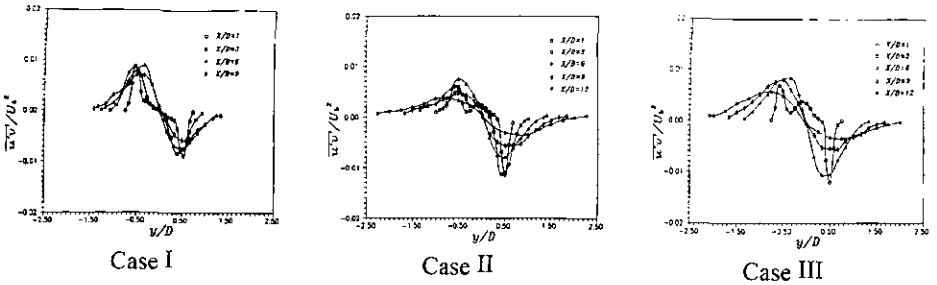

Fig. 11 Reynolds shear stress profiles for Case Ⅰ, Ⅱ, Ⅲ

distribution of 90° bend pipe at y/D=1, 3, 6, 9, and 12. The distribution is no longer symmetric along the x-axis due to skewness of mean velocity distribution. Larger values of $\overline{u'v'}$ occur in the region of high mean shear.

It may also indicate the high degree of development of turbulence and the "nearequilibrium" state which is due to the lack of strong energy production, usually driven by large scale organized structures. Of course, this point can't be substantiated at the present and further study is needed into the organized structure of flow. The location of maximum value of shear stress is shifted toward the outer region of the jet. At x/D =1, the maximum positive value of shear stress is 0.0115 at y/D=0.6678 and the maximum negative value is −0.0059 at y/D=0.5008, respectively. The maximum value of shear stress is decreased with the downstream distance because the effect of initially skewed mean velocity decreases. The point of zero shear stress is also shifted toward the x-axis and stays at y/D=0 after 7 diameters indicating a tendency toward a symmetric turbulent flow structure. However, the distribution of $\overline{u'v'}$ is not yet symmetric at this location. At x/D =9, the distribution is symmetric about x-axis which provides an evidence that the flow is reaching symmetric conditions from initial three-dimensional perturbation.

Case Ⅲ illustrates the shear stress distribution for the different axial locations. At x/D=1, the positive and negative maximum values of shear stress are increased slightly compared to those of 90° bend pipe case. At the same axial location, the location of maximum ($\overline{u'v'}$) is found to be y/D= 0.5008 which is about the same for 90° bend pipe. The maximum value on the positive y-direction increases up to x/D=4. On the other hand, the maximum value on the negative y-direction does not change. After 6 diameters, the maximum positive value of shear stress is rapidly decreased, while the maximum negative value is decreased slowly. The distribution is symmetric after 10 diameters also in Case Ⅲ. Therefore, it may be assumed that the effects of initially skewed mean velocity are overcome beyond 10 diameters from the jet exit.

3.4 Vorticity

In order to calculate the vorticity at each data point, measurements are taken on the symmetric plane and the increments in x and y directions are kept constant. The vorticity component normal to the measurement plane is defned as

$$\Omega_z=\frac{D}{U_b}\left(\frac{\Delta V}{\Delta x}-\frac{\Delta U}{\Delta y}\right)$$

Case Ⅰ in Fig. 12 shows the vorticity distribution of the straight pipe at x/D=1, 3, 6, and 9. At x/D=1, the maximum vorticity of inner side of a jet is −0.248 and has approximately the same value of its counterpart of outer side, which is 0. 252. The positions of positive and negative maximum vorticity show symmetrical distribution. Figure 12 also shows the vorticity distributions of Case Ⅱ and Case Ⅲ. In Case Ⅱ, an asymmetric profile is shown at x/D=1 because of skewed streamwise mean velocity. However, the asymmetric distributions become symmetric after x/D =7. The point of minimum vorticity stays at y/D =0 for x/D>7 which is in accord with the result of Reynolds shear stress. This result indicates that

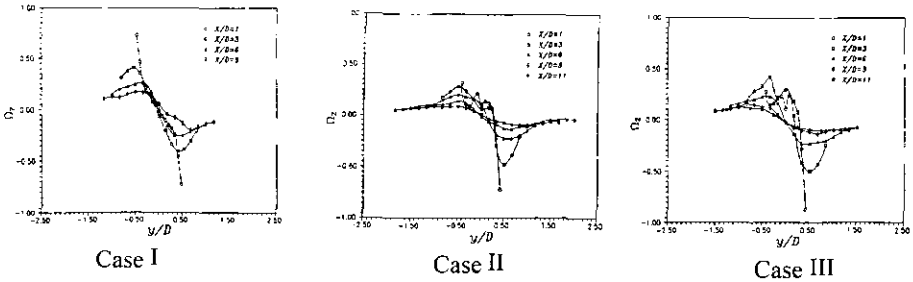

Fig. 12 Vorticity profiles for Case Ⅰ, Ⅱ, Ⅲ

the profile of streamwise mean velocity becomes symmetric and the jet approaches a fully developed turbulent flow state. The value of the positive maximum vorticity at x/D=11 which is 0.0897, is approximately the same magnitude of the maximum negative vorticity which is −0.0916.

In Case Ⅲ, the maximum positive and negative values of vorticity are larger in comparison that with Case Ⅱ. The negative maximum value at x/D=1 is increased by about 20% as compared to the value of Case Ⅱ. The profile of negative vorticity has more rapid decay rate than the positive vorticity, but the decay rates of both sides become equal after x/D=7. Moreover, the magnitude and the entire profile of two distributions in Case Ⅱ and Case Ⅲ are approximately the same after x/D=9.

4. Conclusions

The present investigation is conducted to study the near field structure of asymmetric, incompressible turbulent jets. The asymmetry of the exit profile is controlled by adjusting the circular pipes with a upstream bend of the exit. The radius of curvature of the pipe bend is kept constant. Mean velocity, turbulence intensity, shear stress, and vorticity data are presented and compared to those obtained from an axisymmetric round jet.

The results show that the near field structure of turbulent jet is significantly modified by the initially asymmetric mean velocity distribution and the decay rate of the maximum mean velocity is increased when the skewness level of the exit profile is increased. For the distribution of turbulence intensity, a strong asymmetry is obtained because of the imbalanced mean shear distribution in Case Ⅱ and Ⅲ. The values of turbulence intensity in Case Ⅲ are greater than those in Case Ⅱ. The distribution of turbulent shear stress is also influenced strongly by skewness of the velocity profile. The profile of Reynolds shear stress becomes symmetric at approximately 9 and 10 diameters downstream from the exit for the 90° bend and 160° bend jet cases, respectively. The profiles of streamwise mean velocity also become symmetric at x/D=9 and 10. The vorticity distributions in Case Ⅱ and Ⅲ are also symmetric after x/D=7 and 9. Although there is no information on the jet flow field after 12 diameters, it seems that the influence of the initial skewness of mean velocity almost disappears beyond pipe diameters from the exit plane.

The experimental results indicate that the asymmetric jets have significantly different mean and turbulent velocity structures than those for the axisymmetric jet, especially in the initial jet development region. The mean shear distributions are also modified due to skewness of the initial mean velocity profile. As the level of skewness increases, the structure of turbulent jet is further modified. Therefore, the results may lead to the possibility of using the asymmetric skewed turbulent jet as a device to enhance the mixing control mechanism.

References

Birch, A. D., Brown, D. K., Dodson, M. G., and Thomas, J. R., 1978, "The Turbulent Concentration Field of a Methane Jet," *J. Fluid Mech.* 88, pp. 431～449.

Bradbury, L. J. S., 1965, "The Structure of a Self-preserving Turbulent Plane Jet," *J. Fluid Mech. 23*, pp. 31～64.

Chevray, R. and Tutu, N. K., 1978, "Intermittency and Preferential Transport of Heat in a Round Jet," *J. Fluid Mech.* 88, pp. 133～160.

Dimotakis, P. E., Miake-lye, R. C., and Papantoniou, D. A., 1983, "Structure and Dynamics of Round Turbulent Jets," *Phys. Fluids*, 26, pp. 3185～3192.

Gibson, M. M., 1963, "Spectra of Turbulence in a Round Jet," *J. Fluid Mech.* 15, pp. 161～173.

Hussain, F. and Husain, H., 1989, "Elliptic Jet, Part 1. Characteristics of Unexcited and Excited Jets," *J. Fluid Mech.* 208, pp. 257～320.

Hussain, F. and Tso, J., 1989, "Organized Motions in a Fully Developed Turbulent Axisymmetric Jet," *J. Fluid Mech.* 203, pp. 425～448.

Krothapalli, A., Baganoff, D. and Karamcheti, K., 1981, "On the mixing of a Rectangula," *J. Fluid Mech.* 107.

Kwon, Y. P. 1998, "Instability of High-Speed

Imiging Jets. Pt. 1 Plane Jets," *Transaction of the Korean Society of Mechanical Engineers B*, Vol. 22, No. 4, pp. 425~458.

Namer, I., and Otugen, M. V., 1988, "Velocity Measurement in a Plane Turbulent Air Jet at Moderate Reynolds Numbers," *Exper. Fluids, 6*, pp. 387~399.

Oosthuizen, P. H., 1983 "An Experimental Study of Low Reynolds Number Turbulent Circular Jet Flow," *ASME paper presented at ASME Applied Mechanics, Bioengineering and Fluids Engineering Conference*, Houston/TX, USA, June 20-22. pp. 83-fe-36.

Papanicolaou, P. N. and List, E. J., 1988, "Investigation of Round Vertical Turbulent Buoyant Jets," *J. Fluid Mech.* 195, pp. 341~391.

Ricou, F. P. and Spalding, D. B., 1990, "Measurements of Entrainment by Axisymmetrical Turbulent Jets," *AIAA. J.*, 28 pp. 1025~1032.

Rockwell, D. O., and Niccols, W. O., 1972. "Natural Breakdown of Planar Jet," *Trans. of ASME*, pp. 720~730.

Sforza, P. M., Stieger, M. H., and Trantacoste, N., 1966, "Studies on Three-dimensional Viscous Jets," *AIAA J.*, 4, pp. 800~806.

Shlien, D. J., 1987, "Observation of Dispersion of Entrained Fluid in the Self-preserving Region of a Turbulent Jet," *J. Fluid Mech.* 183, pp. 163~173.

Townsend, A. A., 1956, "The Structure of Turbulent Shear Flow," Cambridge University Press.

Townsend, A. A., 1966, "The Mechanism of Entrainment in Free Turbulent Flows," *J. Fluid Mech.* 26, Part 4, pp. 689~715.

Trentacoste, N. and Sforza, P. M., 1967, "Further Experimental Results for Three-dimensional Free Jets," *AIAA J.*, 5, pp. 885~891.

Trentacoste, N. and Sforza, P. M., 1968, "Some Remarks on Three-dimensional Wakes and Jets," *AIAA J.*, 6, pp. 2454~2456.

Yu, Y. J. and Kim. Y. T., 1996, "Effects of Nozzle on LBB Evaluation for Small Diameter Nuclear Piping," *Transaction of the Korean Society of Mechanical Engineers A*, Vol. 20, No. 6, pp. 1872~1881.